The EMBO Journal (2006) 25, 3843–3855 | © 2006 European Molecular Biology Organization | All Rights Reserved 0261-4189/06
www.embojournal.org

THE EMBO JOURNAL

Nebulin regulates thin filament length, contractility, and Z-disk structure *in vivo*

Christian C Witt[1], Christoph Burkart[1], Dietmar Labeit[1], Mark McNabb[2], Yiming Wu[2], Henk Granzier[2] and Siegfried Labeit[1,*]

[1]Institute for Anaesthesiology and Intensive Care, University Hospital Mannheim, Mannheim, Germany and [2]Department of VCAPP, Washington State University Pullman, WA, USA

The precise assembly of the highly organized filament systems found in muscle is critically important for its function. It has been hypothesized that nebulin, a giant filamentous protein extending along the entire length of the thin filament, provides a blueprint for muscle thin filament assembly. To test this hypothesis, we generated a KO mouse model to investigate nebulin functions *in vivo*. Nebulin KO mice assemble thin filaments of reduced lengths and ~15% of their Z-disks are abnormally wide. Our data demonstrate that nebulin functions *in vivo* as a molecular ruler by specifying pointed- and barbed-end thin filament capping. Consistent with the shorter thin filament length of nebulin deficient mice, maximal active tension was significantly reduced in KO animals. Phenotypically, the murine model recapitulates human nemaline myopathy (NM), that is, the formation of nemaline rods combined with severe skeletal muscle weakness. The myopathic changes in the nebulin KO model include depressed contractility, loss of myopalladin from the Z-disk, and dysregulation of genes involved in calcium homeostasis and glycogen metabolism; features potentially relevant for understanding human NM.

The EMBO Journal (2006) **25,** 3843–3855. doi:10.1038/sj.emboj.7601242; Published online 10 August 2006
Subject Categories: proteins; molecular biology of disease
Keywords: nebulin; nemaline myopathy; thin filament; titin; Z-disk

Introduction

Regular sarcomeric assemblies are comprised of the motor protein myosin that is organized into thick filaments and of actin monomers that are assembled into thin filaments, both of which are highly uniform in length (for a review, see Clark *et al*, 2002). The precision of assembly achieved *in vivo* has intrigued cell biologists and requires the action of capping proteins that control the addition of actin monomers to thin filaments: tropomodulin (Tmod) at the pointed (or H-zone) end (Gregorio *et al*, 1995; Littlefield *et al*, 2001; McElhinny *et al*, 2001) and CapZ at the barbed (or Z-disk) end (Schafer and Cooper, 1995). Although these molecules may explain why the filaments stop growing, it is hard to envision how they specify filament length. A prime candidate for a thin filament ruler is nebulin, because nebulin extends along the entire length of the thin filament (Wang and Wright, 1988), and its primary structure is composed of ~185 α-helical 35-residue repeats, termed M1 to M185 (Labeit *et al*, 1991; Labeit and Kolmerer, 1995b; Wang *et al*, 1996). Each of these 185 repeats is a potential actin binding-motif as suggested by *in vitro* studies (Wang *et al*, 1996). Finally, nebulin isoform size and thin filament lengths are correlated in different types of skeletal muscle tissues (Kruger *et al*, 1991; Labeit *et al*, 1991), further supporting the hypothesis that nebulin functions as a molecular ruler for the thin filament (for a review, see Trinick, 1994).

Nebulin transcripts can also be amplified by RT–PCR from other tissues such as heart, liver, and neuronal cells (McElhinny *et al*, 2003). In the case of myocardium, low-level expression of nebulin has been reported (Kazmierski *et al*, 2003), and its knockdown by a recent RNAi approach resulted in highly elongated thin filaments (McElhinny *et al*, 2005). This suggests that nebulin might also play a role in thin filament length regulation in the myocardium. These observations resulted in the proposal that expression of diverse nebulin splice isoforms might control thin filament lengths in diverse tissues (McElhinny *et al*, 2003), thereby possibly accounting for actin filament length variations ranging from ~20 nm (erythrocyte membrane) to ~1.3 μm in skeletal muscle. However, a problem of the ruler hypothesis is that nebulin is only present in skeletal muscle at sufficient levels to match the stoichiometry of the thin filament, that is, in skeletal muscle nebulin corresponds to about ~2–3% of the total myofibrillar proteins expressed, corresponding to ~2 molecules per thin filamanent (Pfuhl *et al*, 1994; Wang *et al*, 1996). Therefore, other models have been proposed in which dynamic interactions of capping factors, in particular tropomodulins, set actin filament lengths in a statistical fashion by the control of a dynamic equilibrium (for details, see Littlefield *et al*, 2001 and references therein). In addition to thin filament length control, *in vitro* studies with expressed nebulin fragments suggest that nebulin might have a regulatory role in muscle contraction: expressed nebulin fragments were found to inhibit actomyosin ATPase activity and the sliding velocity of actin over myosin in *in vitro* motility assays (Root and Wang, 1994).

Previous insights into the *in vivo* function of nebulin have been limited by the unavailability of genetic models. For example, current *in vitro* and *in vivo* expression systems make it impossible to express full-length nebulin due to its giant size (Mw 800 kDa). The RNAi knockdown of nebulin transcripts in skeletal myoblasts blocked myofibrillogenesis, making it impossible to obtain functional data from skeletal cells (McElhinny *et al*, 2005). To test the functional role(s) of

*Corresponding author. Institute for Anaesthesiology and Intensive Care, University Clinic Mannheim, Theodor-Kutzer-Ufer 1-3, Mannheim 68167, Germany. Tel.: +49 621 3831625; Fax: +49 621 3831971; E-mail: Siegfried.Labeit@anaes.ma.uni-heidelberg.de

Received: 10 January 2006; accepted: 26 June 2006; published online: 10 August 2006

nebulin *in vivo*, we inactivated the murine nebulin gene (NEB) by a targeted disruption. We obtained NEB KO mice viable up to postnatal day 20, and that assemble nebulin-free myofibrils, demonstrating that nebulin is not required for myofibrillogenesis. NEB KO mice develop progressive weakness and skeletal muscle myopathy. Their unaffected cardiac myocytes suggests that other mechanisms determine actin filament lengths in cardiac tissues. The NEB KO mouse allows us for the first time to functionally compare wild type (wt) and nebulin free skeletal myofibrils and to gain detailed insights into nebulin's myofibrillar *in vivo* functions. Our work shows that in skeletal muscle, nebulin's functions extend beyond pointed-end thin filament length control as previously suspected, and include control of thin filament barbed-end capping, Z-disk structure, and contractility.

Results

Generation of nebulin null mice with severe skeletal muscle myopathy

We inactivated the murine nebulin gene by targeting its 5′ UTR region and exon 1 via homologous recombination, thereby removing nebulin's cap site, TATA-box, and its putative Tmod-binding aminoterminal domain (see Figure 1A and B). Mice heterozygous for this allele (ht mice) were viable and fertile and had the same nebulin expression level as wt mice (Figure 2A, left). In contrast, nebulin was absent in the skeletal muscles of mice homozygous for the targeted allele (see Figure 2A, right). Insertions into the genome by homologous recombination potentially can activate aberrant splice pathways, thereby causing the removal of the targeting cassette, the expression of a truncated protein, and partial rescue (e.g., see Witt *et al*, 2001). Therefore, in addition to testing antibodies directed to nebulin's N-terminus (Figure 2A), we performed Western blot studies with two different antibodies directed to nebulin's C-terminal region. We analyzed both the molecular weight regions above 200 kDa on agarose gels, and the 20–200 kDa on 10% acrylamide gels. Results with three different antibodies directed to either nebulin's N- or C-terminal epitopes indicated the absence of nebulin (Figure 2B). The homozygous NEB KO mice were already growth-retarded at day 1 after birth (see Figure 3B). About 90% of the NEB KO mice die within the first 2 weeks after birth, the remaining ~10% of animals die during their third week. NEB KO mice develop a stiff gait and kyphosis (Figure 3A and B). They are able to walk up to week 3 (see Supplementary videos: 'Nebulin mouse13d' and 'Nebulin mouse 18d'. As a comparison, a heterozygous healthy littermate is shown). Between day 10 and 20, nebulin KO mice develop progressive muscle weakness as indicated by their inability to climb, hold their weight when clinging to a spatula, and inability to keep their eyes open (Figure 3A and Supplementary videos: 'Nebulin mouse13d' and 'Nebulin mouse 18d').

Dysregulation of sarcolipin, S100A4/A9, desmoplakin, CARP/ankrd2 expression in NEB KO mice

To gain molecular insights into the disease mechanisms causing myopathy in the NEB KO mice, we surveyed their

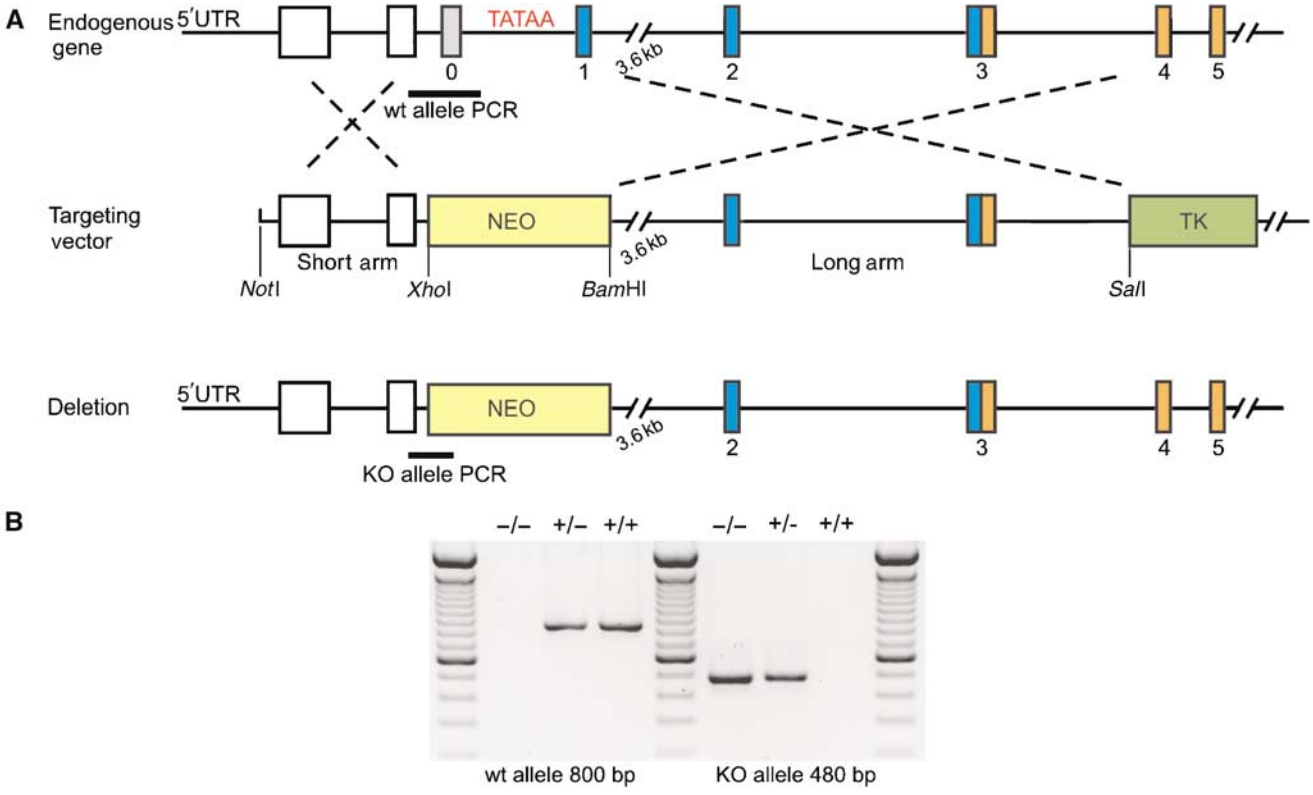

Figure 1 Generation of NEB KO mice. (**A**) Schematic description of the NEB KO targeting strategy. Exons 0 and 1 of murine Nebulin 5′ region were replaced by a Neomycin cassette (NEO). NEO and thymidin kinase (TK) were used for positive and negative selection of ES cells. The short and the long arm were generated by long PCRs. For the genomic sequence of murine nebulin, see Kazmierski *et al* (2003). (**B**) Genotyping of NEB KO, wt and heterozygous mice. KO, wt and heterozygous animals were genotyped by two different PCRs. KO animals show a 480 bp band and no 800 bp band, wt animals show no 480 and a 800 bp band, heterozygous animals show both bands.

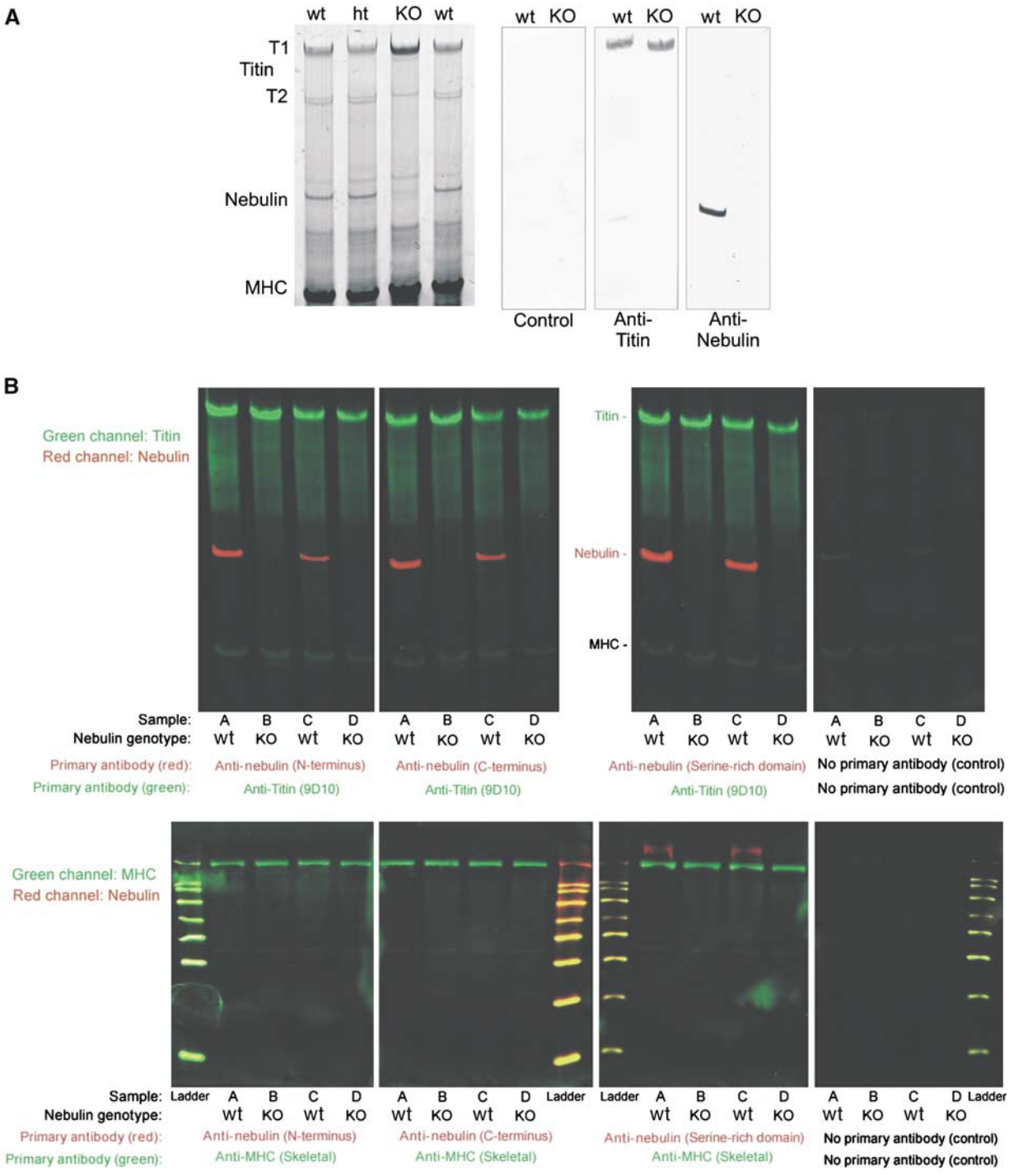

Figure 2 Skeletal myofibrillar protein expression in NEB KO and wt mice. (**A**) Left: SDS agarose gel reveals normal myofibrillar proteins in quadriceps muscle in the KO mice, except for the absence of a ~800 kDa protein. Quantitative densitometry revealed that the expression level of titin is the same in wt, ht, and KO animals (data not shown). Right: Western blots reveal normal expression of titin but absence of nebulin in KO. (**B**) Analysis of nebulin and titin expression by two-color Western blots in NEB KO and wt mouse skeletal muscles. Quadriceps muscles from four mice were tested with three different nebulin antibodies. The four samples under investigation were (lanes marked A) 10-day-old wt, (lanes marked B) 10-day-old NEB KO (lanes marked C) wt of 5-day-old wt, and (lanes marked D) 5-day-old NEB KO. Antibodies to titin and myosin heavy chain (MHC) were used as positive controls. Top: Screen for nebulin expression in the molecular mass region between titin and MHC. Bottom: Proteins smaller than MHC were also tested with nebulin antibodies. Nebulin was not detectable in NEB KO mice (M_r standards listed from small to large: 20, 30, 40, 50, 60, 80, 100, and 120 kDa).

transcriptomes using affymetrix gene arrays. This identified 40 differentially expressed genes that were more than 10-fold upregulated in quadriceps skeletal muscles of NEB KO animals (see EBI array express accession E-MEXP-733; selected genes are shown in Figure 3C). Of these 40 genes we analyzed by RT–PCR desmoplakin (DSP) (to clarify if this cardiac gene is also expressed in skeletal muscle), sarcolipin (as a member of the calcium regulating proteins), agouti-related protein (because of its growth-factor like properties), and CARP, its homolog ankrd2, and CSRP3/MLP (because of

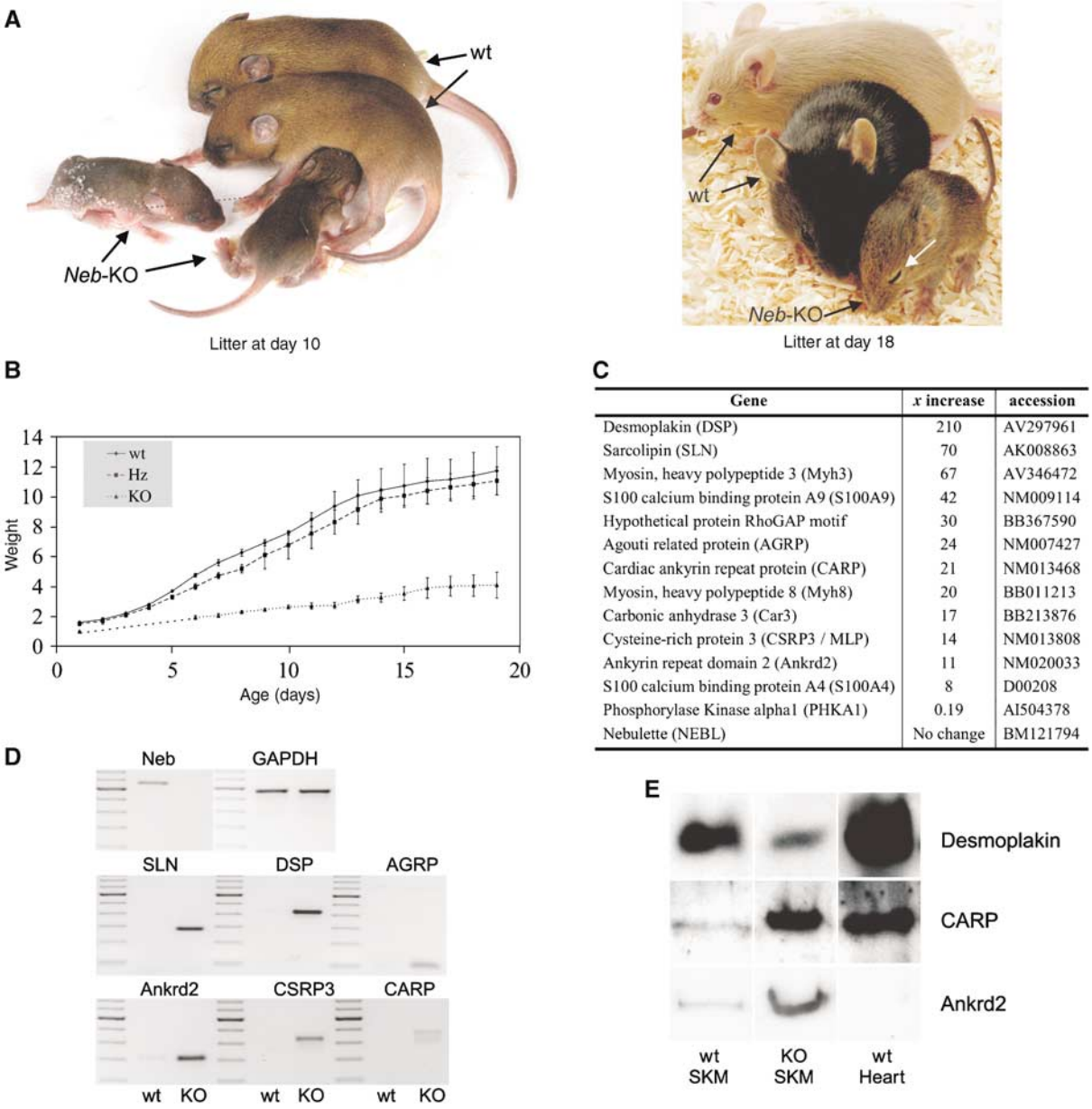

Gene	*x* increase	accession
Desmoplakin (DSP)	210	AV297961
Sarcolipin (SLN)	70	AK008863
Myosin, heavy polypeptide 3 (Myh3)	67	AV346472
S100 calcium binding protein A9 (S100A9)	42	NM009114
Hypothetical protein RhoGAP motif	30	BB367590
Agouti related protein (AGRP)	24	NM007427
Cardiac ankyrin repeat protein (CARP)	21	NM013468
Myosin, heavy polypeptide 8 (Myh8)	20	BB011213
Carbonic anhydrase 3 (Car3)	17	BB213876
Cysteine-rich protein 3 (CSRP3 / MLP)	14	NM013808
Ankyrin repeat domain 2 (Ankrd2)	11	NM020033
S100 calcium binding protein A4 (S100A4)	8	D00208
Phosphorylase Kinase alpha1 (PHKA1)	0.19	AI504378
Nebulette (NEBL)	No change	BM121794

Figure 3 Phenotype of NEB KO mice. (**A**) Mice homozygous for a targeted disruption of nebulin's 5′ UTR region and exon 1 are reduced in size, and have severe muscle weakness as indicated by ptosis (white arrow in right picture). (**B**) Weight curve. NEB KO mice have a reduced weight over the full postnatal age range that was tested (starting at day one). KO mice and wt animals already differ in weight at day 1 by about 35%. Around day 16, KO mice reach a maximal weight of 3–4 g and they die before day 20. Mice heterozygous for the targeted disruption (ht) and wt animals do not differ in weight during postnatal development (data obtained from two litters with three animals per group). (**C**) Left: Gene expression profiling of quadriceps muscle at days 13 and 18 using affymetrix arrays identifies among others 12 known genes that are 8–210-fold upregulated, and among others one gene that is five-fold downregulated (for a full description of all differentially expressed genes, see EBI array express accession E-MEXP-733). (**D**) Semiquantitative RT–PCR analysis of independent nebulin KO animals mice (day 14) confirms the upregulation of sarcolipin (SLN), DSP, agouti-related protein (AGRP), ankrd2, muscle LIM protein (CSRP3), and CARP. (**E**) Western blots show that CARP and ankrd2 are upregulated in NEB-KO quadriceps, whereas DSP is downregulated.

their direct association with the myofibril and their stretch-dependent regulation (Knoell *et al*, 2002; Miller *et al*, 2003)). All genes were upregulated, by 210-, 70-, 24-, 21-, 14-, and 11-fold (same order as listed genes). This RT–PCR analysis confirmed the affymetrix gene array results (see Figure 3D). Those genes that are dramatically upregulated on the transcriptional level and for which antibodies are available, were also analyzed by Western blots. For CARP and ankrd2, Western blots with specific antibodies confirmed their strong upregulation in skeletal muscle NEB KO tissues (see Figure 3E), consistent with the upregulation of their transcript. For DSP when using the sensitive ECL-based detection system (Vectastain), DSP was detected in skeletal muscle tissues and its expression level was reduced in KO mice (Figure 3E). Currently we speculate that the reduced presence of DSP protein induces a compensatory response that gives rise to the increased DSP transcript (Figure 3C and D). In cardiac muscle, DSP is an essential linker protein in desmosomes ('spot welds' between cells that are anchored intracellularly to the cytoskeleton (Getsios *et al*, 2004)), whereas,

to our knowledge, DSP in skeletal muscle has not been described. Possibly, this is due to the low levels of DSP expressed in skeletal muscle and its co-migration with MHC on regular SDS–PAGE gels (unpublished data). Future studies are required to determine the function of DSP in skeletal muscle and how this function relates to the presence of nebulin.

Loss of thin filament length control and pointed end capping in NEB KO skeletal muscle tissues

We structurally and functionally characterized skeletal myofibrils from nebulin KO and wt mice using electron microscopy (EM), immunoelectron microscopy (IEM), and immunofluorescence confocal microscopy (IF). Selected mice were 10–15 day old, because NEB KO animals at that age have reached their maximal weight and are still able to walk and nurture (Figure 3B). Consistent with the Western blot data (Figure 2A), IEM and IF detected the absence of N- and C-terminal ends of the nebulin filament (Figure 4A). IF with control antibodies such as α-actinin (Z-disk), and MHC (A-band) indicated that both wt and NEB KO myofibrils are well organized with regular cross-striations (Figure 4A and B). However, the thin filament capping proteins, CapZ and tropomodulin-1 (Tmod1) (Gregorio *et al*, 1995; Schafer and Cooper, 1995; Littlefield *et al*, 2001; McElhinny *et al*, 2001), and myopalladin (a nebulin ligand as predicted from *in vitro* binding studies, see Bang *et al* (2001)) were affected in the NEB KO. Myopalladin strongly labelled the Z-disk in wt mice, and this labelling was greatly reduced in the NEB KO (Figure 4C). CapZ labelling was more broadly distributed and less intense in Z-disks in NEB KO myofibrils (Figure 4D). IEM with Tmod1 showed a weak epitope at the edge of the H-zone in wt that was absent in the NEB KO (data not shown). IF with Tmod1 resulted in wt in an intense doublet in the center of the sarcomere. Labelling was much reduced and was translocated towards the Z-disk in the NEB KO (Figure 4E). Western blots and array data suggest that expression levels of Tmod1, CapZ, and myopalladin were not altered, supporting that their myofibrillar targeting, and not their expression is altered in the NEB-KO mice (data not shown).

EM revealed that the overall sarcomeric structure of KO animals was similar to that of wt animals (Figures 4A, bottom and 5A–C), suggesting that nebulin is not required for myofibrillogenesis. An unusual ultrastructural feature was the absence of H-zones in KO animals (Figure 5A and B). Densitometry scans along the longitudinal axis revealed in KO animals a gradual reduction in intensity (Figure 5B), in contrast to the step-like reduction in wt animals (Figure 5C). This indicates that in wt muscle, thin filaments are of a defined length, but that this is not the case in KO muscle. To measure thin filament lengths more directly, we labelled skinned muscle fibers with the actin-binding protein phalloidin, conjugated to biotin, followed by streptavidin-coated gold beads that were silver-enhanced (Figure 5D). Consistent with a uniform thin filament length distribution in control muscle, silver grains were evenly distributed up to 1.2 μm distance from the edge of the Z-disk (Figure 5E, bottom left). In contrast, in KO sarcomeres, grain distribution suggests that thin filaments are shorter and range in length from ~0.4 to 1.2 μm (Figure 5E, bottom right). These findings are consistent with the absence of H-zones and the gradual reduction of A-band density.

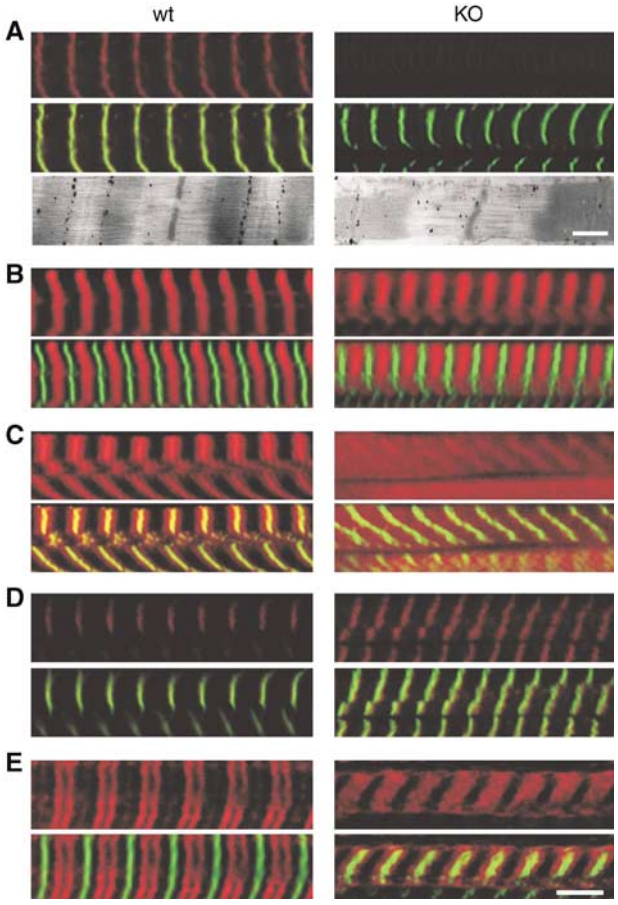

Figure 4 Structural studies on skeletal myofibrils from wt and NEB KO mice. Confocal microscopy of quadriceps muscle fibers. All fibers were labelled with alpha-actinin (green) and in addition with an antibody of interest (in red), with spatially overlapping epitopes resulting in a yellowish color. In each panel the top section shows the red channel and the bottom section the red and green channels combined. Specific antibodies were (**A**) nebulin-SH3, (**B**) myosin heavy chain (MHC), (**C**) myopalladin, (**D**) CapZ, and (**E**) Tropomodulin 1 (Tmod1). Additionally electron micrograph labelled with antibody directed to nebulin's N-terminus is shown at the bottom of (A). (A) Results indicate absence of nebulin's C-terminal (IF) and N-terminal (IEM) epitopes in KO (note in IEM epitope at edge of H-zone in wt and absence of this epitope in KO). (B) MHC labelling is normal in KO mice. (**C**) Myopalladin strongly labels the Z-disk in wt and this is reduced in KO. (D) CapZ labels the Z-disk in wt and labelling is more diffuse in KO. (E) Tmod1 in wt strongly labels a doublet in the middle of the sarcomere. In KO, labelling is much reduced in intensity and labelled zone is now close to Z-disk. Bar: Immunofluorescence: 5 μm, Immuno-EM: 500 nm.

The shorter thin filaments of KO animals predict that maximal active tension will be reduced. We tested this prediction in skinned muscle fibers by measuring active tension at a saturating *p*Ca ($-\log[Ca^{2+}]$ of 4.5, and a sarcomere length (SL) of 2.5 μm. At this SL, overlap between thin and thick filaments is maximal in wt animals but ~50% of maximal in KO animals (as a result of their shorter thin filaments), and maximal active tension is predicted to be reduced accordingly. Consistent with this prediction, measured maximal active tension is significantly reduced (unpaired *t*-test; $P<0.001$) by 54% in KO animals (56.1±3.9

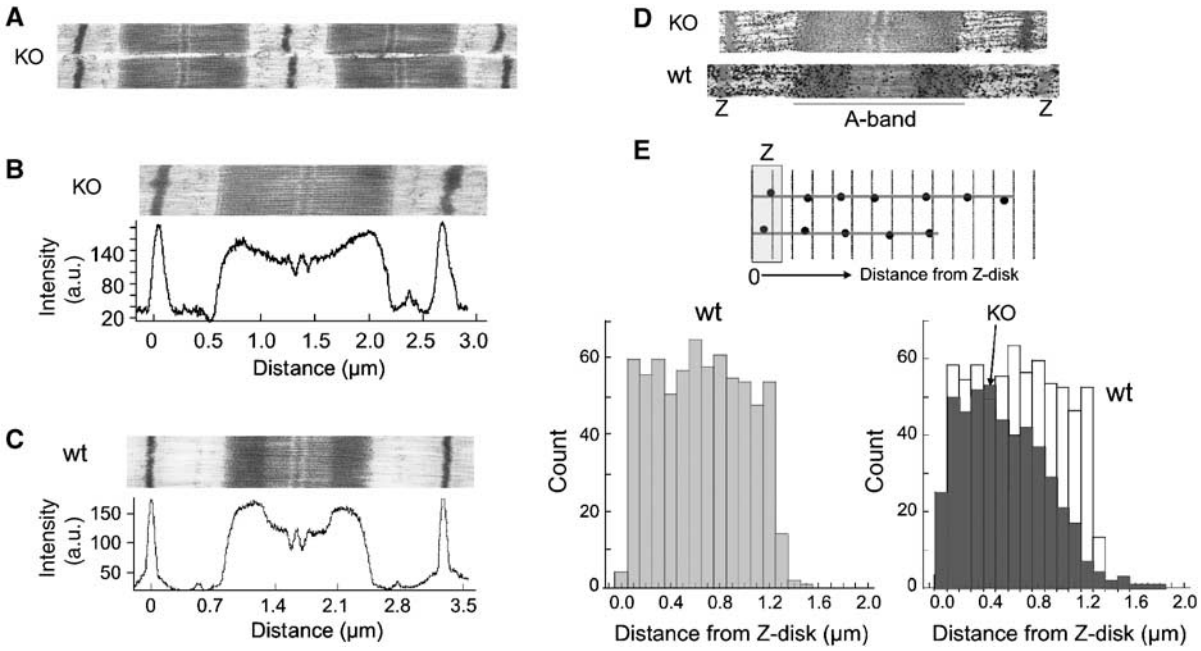

Figure 5 Ultrastructural characterization and thin filament length measurements. Experiments were performed on wt and nebulin KO tibialis cranialis muscle. (**A**) Low magnification micrograph of KO sarcomeres reveals normal structure. (**B**) High magnification micrograph of KO sarcomere. Densitometry scans reveal a continuous reduction of A-band density towards the M-line. (**C**) High magnification micrograph of wt sarcomere. A clear H-zone is present that gives rise to a step-like reduction of A-band density. (**D**) Skinned muscle fibers labelled with phalloidin-biotin, followed by streptavidin-nanogold and silver enhancement. (**E**) Top: Schematic showing how the distance between silver grains and the opposite edge of the nearest Z-disk was measured. Bottom: Histograms of obtained distances are shown for wt (bottom left) and KO superimposed with wt (bottom right). In wt sarcomeres, grain distribution is uniform up to a distance of 1.2 μm. In contrast, in KO tissue, the grain distribution gradually decreases from ~0.4 to ~1.2 μm.

($n=6$) versus 121.6±8.3 ($n=6$); mean±s.e.). Thus, both structural and functional studies support that in the absence of nebulin, thin filament length control is lost and that on average thin filaments are shorter.

Characterization of myocardium of NEB KO mice

Myocardium has been reported to express low levels of nebulin (Kazmierski *et al*, 2003), and moreover, cardiac thin filaments in cultured cardiomyocytes greatly elongate after knockdown of nebulin RNA (McElhinny *et al*, 2005). We therefore used our nebulin KO mice to study how nebulin ablation affects the myocardium. Western blot analysis failed to detect nebulin in left ventricular myocardium from NEB KO mice, similar to our results for skeletal muscle (Figure 6A). However, we were also unable to detect expression of nebulin in cardiac muscle from wt (Figure 6A). As we cannot exclude that the detection methods of our Western blot techniques were insufficiently sensitive to detect low levels of nebulin expression, we also characterized the transcriptome in myocardium of NEB KO mice. We studied wt and NEB KO with the affymetrix array and found that those genes that are strikingly dysregulated in skeletal muscle are not differentially expressed in myocardium. For example, sarcolipin, DSP , and CARP/ankrd2 are expressed at normal levels in cardiac muscle (Figure 6B). The expression of nebulin's cardiac homolog nebulette was also not affected in the NEB KO (Figure 6C). As expected, in skeletal muscle nebulette remained at background levels (see Figures 6C and 3C.) In summary, our results appear not to support nebulin as a ruler molecule for thin filaments in the myocardium (see also Discussion). This contrasts with skeletal muscle tissues where nebulin is required for thin filament length control (Figure 5).

Nebulin is required to fine tune calcium dependent contractility

Previous *in vitro* motility studies with recombinant nebulin fragments indicate that nebulin inhibits the sliding velocity of actin over myosin (Root and Wang, 1994). To test whether nebulin plays a role in regulating actomyosin interaction *in vivo*, we measured tension–*p*Ca ($-\log[Ca^{2+}]$) relations of KO and wt muscle fibers. Monitoring contractions over a wide range of *p*Ca levels revealed that tension develops quickly to a steady plateau (see top of Figure 7A). Tension at *p*Ca 6.25 was significantly increased (unpaired *t*-test; $P=0.01$) in KO animals and the cooperativity of activation (nH) was significantly less (Figure 7A, bottom). Thus, the role of nebulin includes fine-tuning regulation of contraction. To determine if the underlying mechanism is a direct effect of nebulin on actomyosin interaction (such as steric hindrance, analogous to tropomyosin) or an indirect effect, for example, via affecting regulatory components of the thin filament, will require further studies.

Nemaline bodies and wide Z-disks in NEB KO mice recapitulate human NM

Our studies revealed that the Z-disks in NEB KO mice are affected: Z-disk stainings show that CapZ and myopalladin are less intense and more diffuse (Figure 4C and D). In EM micrographs, ~15% of the Z-disks appear unusually wide (Figure 7B). In addition, NEB KO skeletal muscles contain electron-dense Z-disk like bodies that are highly similar to

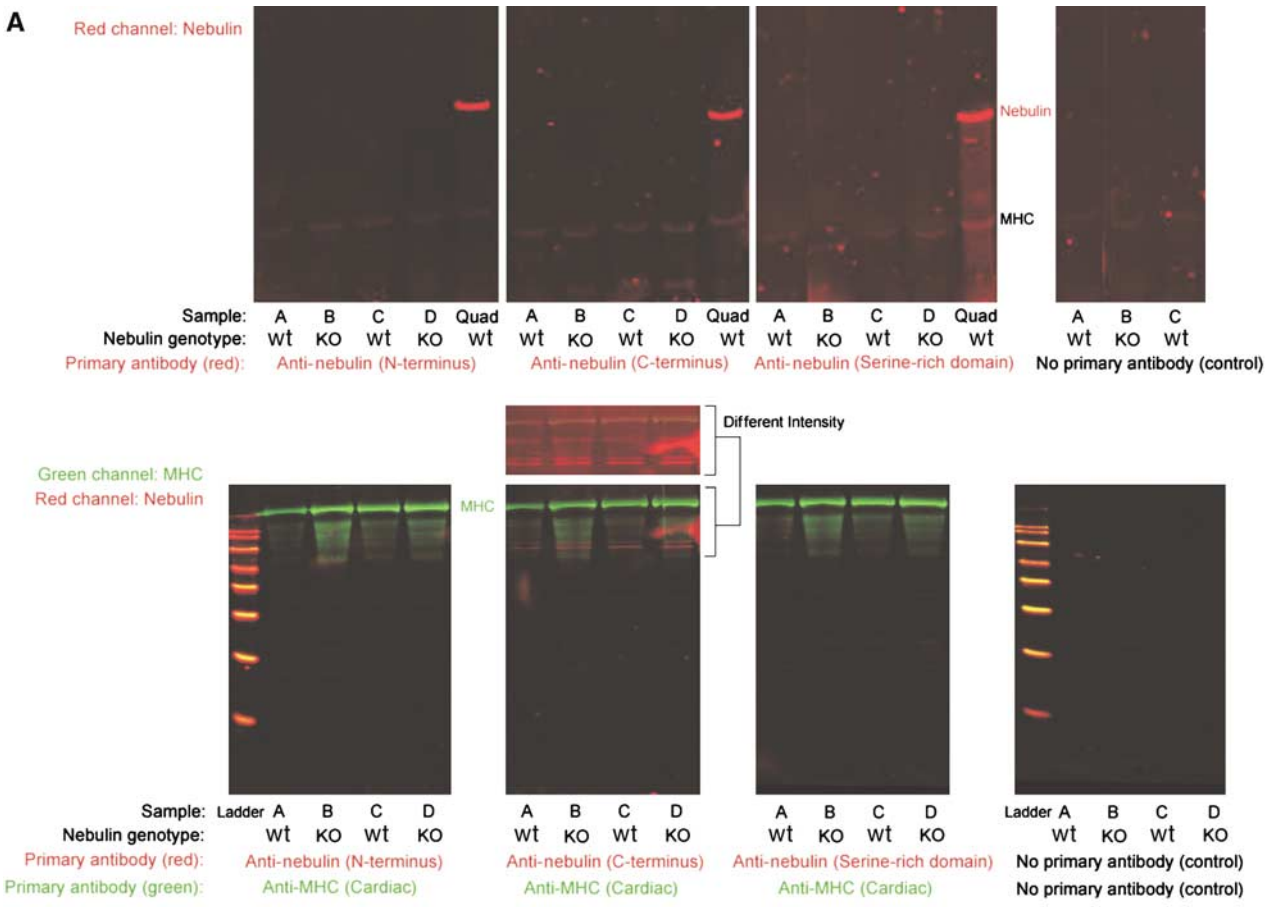

B

Gene	*x* increase in KO	Accession
Desmoplakin (DSP)	No change	AV297961
Sarcolipin (SLN)	No change	AK008863
Myosin, heavy polypeptide 3 (Myh3)	No change	AV346472
S100 calcium binding protein A9 (S100a9)	1.8	NM009114
Hypothetical protein RhoGAP motif	No change	BB367590
Agouti related protein (AGRP)	No change	NM007427
Cardiac ankyrin repeat protein (CARP)	No change	NM013468
Myosin, heavy polypeptide 8 (Myh8)	No change	BB011213
Carbonic anhydrase 3 (Car3)	No change	BB213876
Cysteine-rich protein 3 (CSRP3/MLP)	No change	NM013808
Ankyrin repeat domain 2 (Ankrd2)	No change	NM020033

C

	WT 1 Heart	KO 1 Heart	WT 2 Heart	KO 2 Heart	WT 1 Quad	Accesion
Nebulin	8.3	0.6	0.6	0.7	4867	AI595938
Nebulette	2011	2268	1929	1815	15.2	BM121794

Figure 6 Protein and transcript studies in myocardium of NEB KO mice. (**A**) Two-color Western blots of NEB KO and wt mouse cardiac muscles. Left ventricle muscles from four mice were tested with three different nebulin antibodies. The four samples under investigation were (lanes marked A) 10-day-old wt, (lanes marked B) 10-day-old NEB KO, (lanes marked C) 5-day-old wt, and (lanes marked D) 5-day-old NEB KO. Positive controls were quadriceps (Quad) from a nebulin wt mouse and an antibody to MHC. Top: Screen of nebulin in the molecular mass region between titin and MHC. Bottom: Proteins smaller than MHC were also tested with nebulin antibodies (M_r standards from small to large: 20, 30, 40, 50, 60, 80, 100, and 120 kDa). A separate view of the intensified red channel (anti-nebulin C-terminus) is also shown. This reveals that weak signals are detected with the anti-nebulin antibody but that they are not differential between wt and KO lanes. (**B**) Gene expression profiling in cardiac muscle at day 14 identified no or minimal changes. Shown are 11 of the genes which were highly upregulated in skeletal muscle of nebulin deficient mice (see Figure 3). (**C**) Array data (absolute signal strength) show the *de facto* absence of nebulin transcripts in wt and KO heart for the exons contained on affymetrix array (Mouse Genome 430 2.0). Nebulette is present in wt heart but reveals no differences between wt and KO animals. For comparison the absolute magnitude of skeletal muscle signals is shown.

nemaline-myopathy rod bodies (Figure 7B). Nemaline rod bodies are a diagnostic hallmark of nemaline myopathy (NM) in humans (Sanoudou and Beggs, 2001; Wallgren-Pettersson *et al*, 2004), and derive from pathologically assembled Z-disk proteins. The variation in Z-disk width (Figure 7B and C) observed in the nebulin KO supports a role for nebulin in determining Z-disk widths (see also below). Taken together, perturbed Z-disk widths and altered Z-disk protein compositions suggest that nebulin plays important roles in maintaining physiological Z-disk width and protein composition in skeletal tissues, features that are likely to be functionally important to allow Z-disks to adapt to chronic mechanical loading (Vigoreaux, 1994).

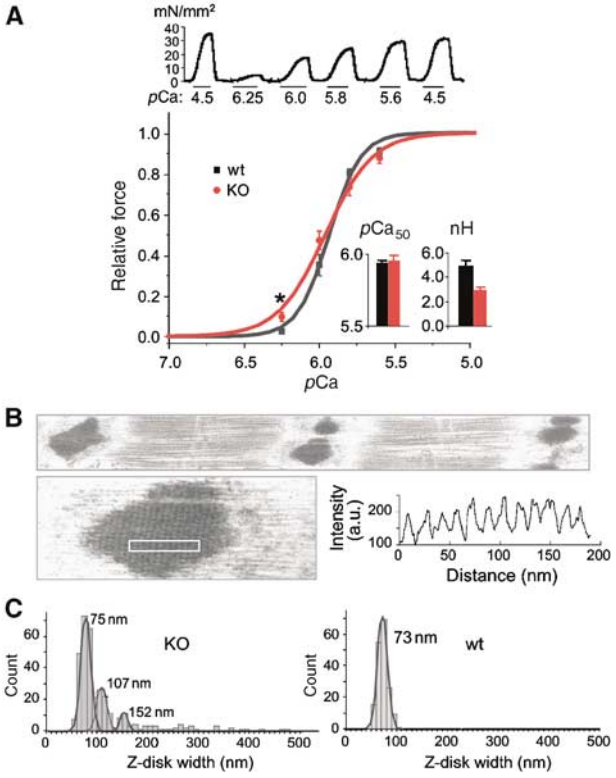

Figure 7 Abnormal calcium sensitivity and Z-disk morphology in nebulin deficient skeletal muscle. Experiments were performed on tibialis cranialis muscle of 1-day-old wt and 14-day-old NEB KO mice. (**A**) Top: Examples of contractions of KO fibers at different *p*Ca levels. Bottom: Tension–*p*Ca curves (mean and SD of 9 KO and 12 wt muscles). KO muscles are more sensitive to calcium at $pCa_{6.25}$ (unpaired *t*-test; $P = 0.01$). No difference in pCa_{50} was found (inset). The slope of the force–*p*Ca relation was more shallow in KO fibers, resulting in a significantly lower (unpaired *t*-test; $P = 0.001$) Hill coefficient, nH (see inset). (**B**) KO muscle fibers contain wide and irregular Z-disks. Bottom: Example of Z-disk like inclusion body in KO muscle. Densitometry of region indicated by white rectangle reveals regular periodicity. Highly irregular and massively widened Z-disks and inclusion-rod like bodies derived from Z-line structures in NEB KO mice resemble the histopathological features observed in human NM (see Morris *et al*, 1990; Sanoudou and Beggs, 2001; Wallgren-Pettersson *et al*, 2004). (**C**) Z-disk width distribution in KO (left) and wt (right) muscle. The majority of Z-disks in KO animals have a width of ~75 nm, which is similar to that of wt animals. Secondary and tertiary peaks are found in the KO histogram at 107 and 153 nm. In addition, a small number of Z-disks are extremely wide, up to ~500 nm.

Nebulin's C-terminus is an integral part of the Z-disc and interacts with titin and CapZ

Z-disks in NEB KO mice are deficient in myopalladin (Figure 4C), consistent with earlier yeast two-hybrid (YTH) studies that demonstrated the interaction of nebulin's C-terminal region with myopalladin (Bang *et al*, 2001). In addition, it has been speculated that nebulin's C-terminal region might interact with CapZ (Schafer and Cooper, 1995), and/or with titin (Politou *et al*, 1998). Interactions made by CapZ are potentially missed by the YTH method, because the heterodimeric CapZ assembles only as a functional protein when both subunits are co-expressed (Soeno *et al*, 1998), whereas interactions with titin (the other ruler molecule implied in Z-disk assembly, see Gautel *et al*, 1996; Young *et al*, 1998) might have been missed by earlier YTH screens since titin's Z-disk region maps ~100 kb upstream of its 3′ end and will be poorly represented in poly-A^+ selected prey clone libraries. We therefore reinvestigated the interaction of nebulin's C-terminal Z-disk region with CapZ by a co-expression approach and with titin's N-terminal Z-disk region. For this, we screened a skeletal cDNA prey library with titin bait clones covering titin's 5′ Z-disk region.

When co-transforming ~200 000 clones with a titin bait containing Z2-Zis1 as insert, a total of 43 interacting prey clones were fished. Of these, 16 prey clones coded for nebulin's C-terminal region. All 16 clones shared as overlapping region the segment M185–Cterm (see Figure 8A). Of the remaining 27 clones, seven coded for α-actinin-2/3, 9 for filamin-A/C, and 11 remain to be characterized (interaction of titin Z2-Zis with α-actinin and filamin is described in more detail in Labeit *et al*, 2006). The interaction of nebulin M185–Cterm was further confirmed on peptide scans (Figure 8B) and using expressed materials for isocalorimetric titrations. Both approaches together demonstrated that a 26-mer proline-rich peptide from titin's Zis1 domain interacts with nebulin's SH3 domain (K_d 4 μM; see Figure 8C). Consistent with the prediction of Politou *et al*, 1998), mutation of

Figure 8 Interaction of nebulin with titin. (**A**) Yeast two-hybrid studies identified the interaction of titin Z2-Zis-1 (coding for residues 103–416 in accession X90568) with nebulin preys (coding for region M185–Cterm). (**B**) A SPOTs blot displaying the titin Z2-Zis-1Ig residues was reacted with expressed nebulin fragment M185–Cterm. Bound nebulin fragment was detected with an antibody-linked ECL assay. The SPOTs 15 and 16 bound nebulin and further fine-map the interacting titin residues to the sequence shown in red/bold. Bottom: Mutation of the proline residues in SPOTs 15 and 16 (indicated as 15m and 16m, respectively) reduced the interaction with nebulin. (**C**) A synthetic peptide corresponding to SPOTs 15/16 from above was used for isocalorimetric titration (ITC). The titin peptide N-QQLPHKTPPRIPPKPKSRSPTPPSIA-C interacted specifically with expressed nebulin fragment M185–Cterm (kDa ~4 μM). (**D**) Z-disk isoforms of titin and nebulin: Top: comparison of titin isoforms expressed in quadriceps (quad) and heart muscle of wt and NEB KO mice by RT–PCR. Quadriceps of wt mice express predominantly titin isoforms with four copies of α-actinin binding Z-repeats (bottom major PCR product). In NEB KO mice (day 14), titin isoforms are shifted towards the six Z-repeat copy isoform (see asterisk) and are more similar to the titin isoform pattern expressed in mouse heart. Below: Comparison of the nebulin splice isoforms expressed in soleus (rich in the 6 Zr titin isoform) and quadriceps (4 Zr titin isoform) detects six nebulin exons that are also differentially expressed. Thus, both titin and nebulin have the largest Z-disk isoform in the soleus muscle, which has the widest Z-disk. See also text.

prolines in the PXXP motif reduced interaction with nebulin (Figure 8B, bottom).

We studied which Z-disk titin and nebulin isoforms are expressed in wt and NEB KO mice. In quadriceps muscle, nebulin deficiency caused an isoform shift from the dominant four Z-repeat copy titin isoform towards the six titin Z-repeat copy-encompassing isoform (see Figure 8D, top). When comparing nebulin isoforms in wt soleus (rich in slow fibers

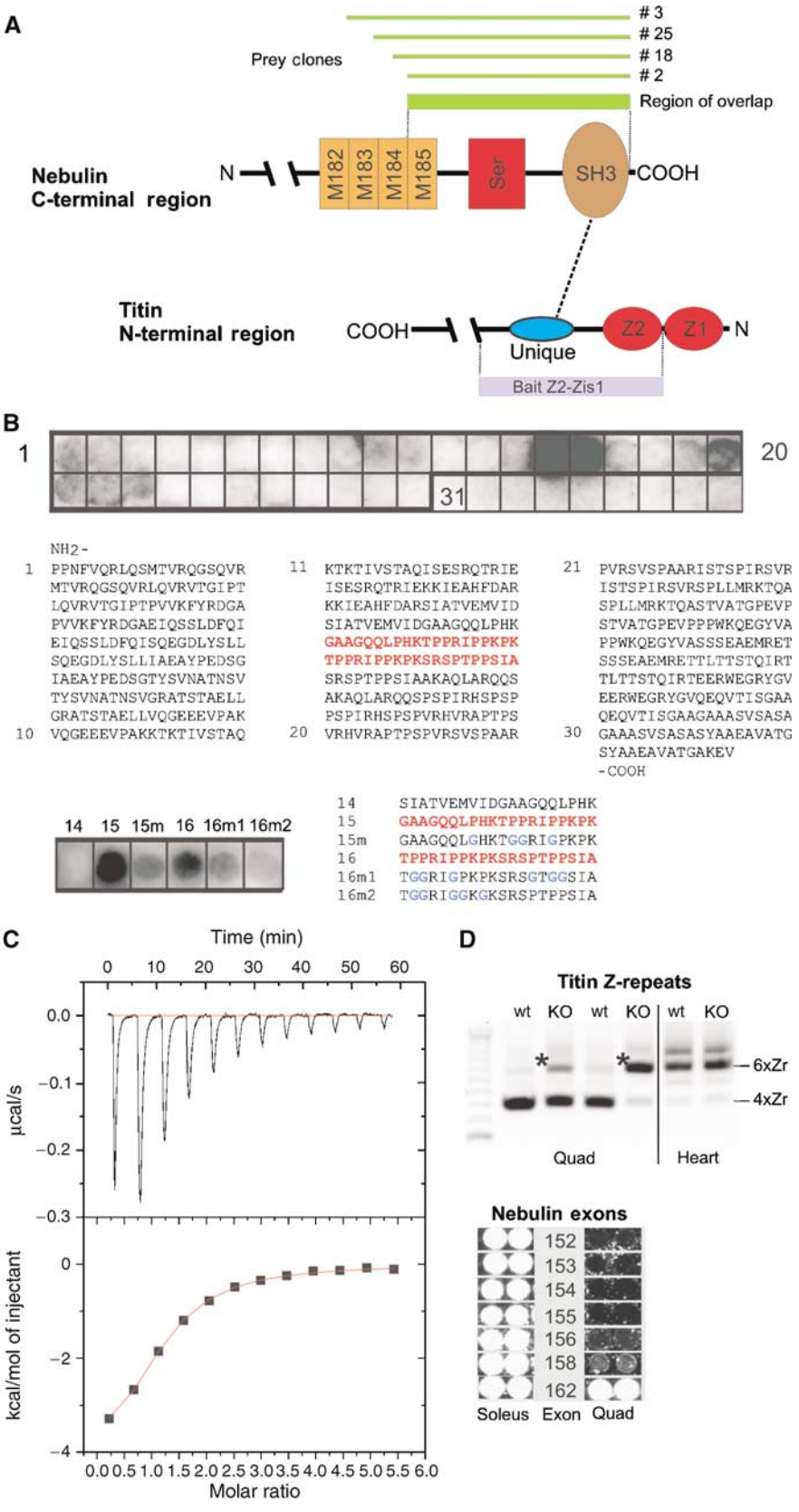

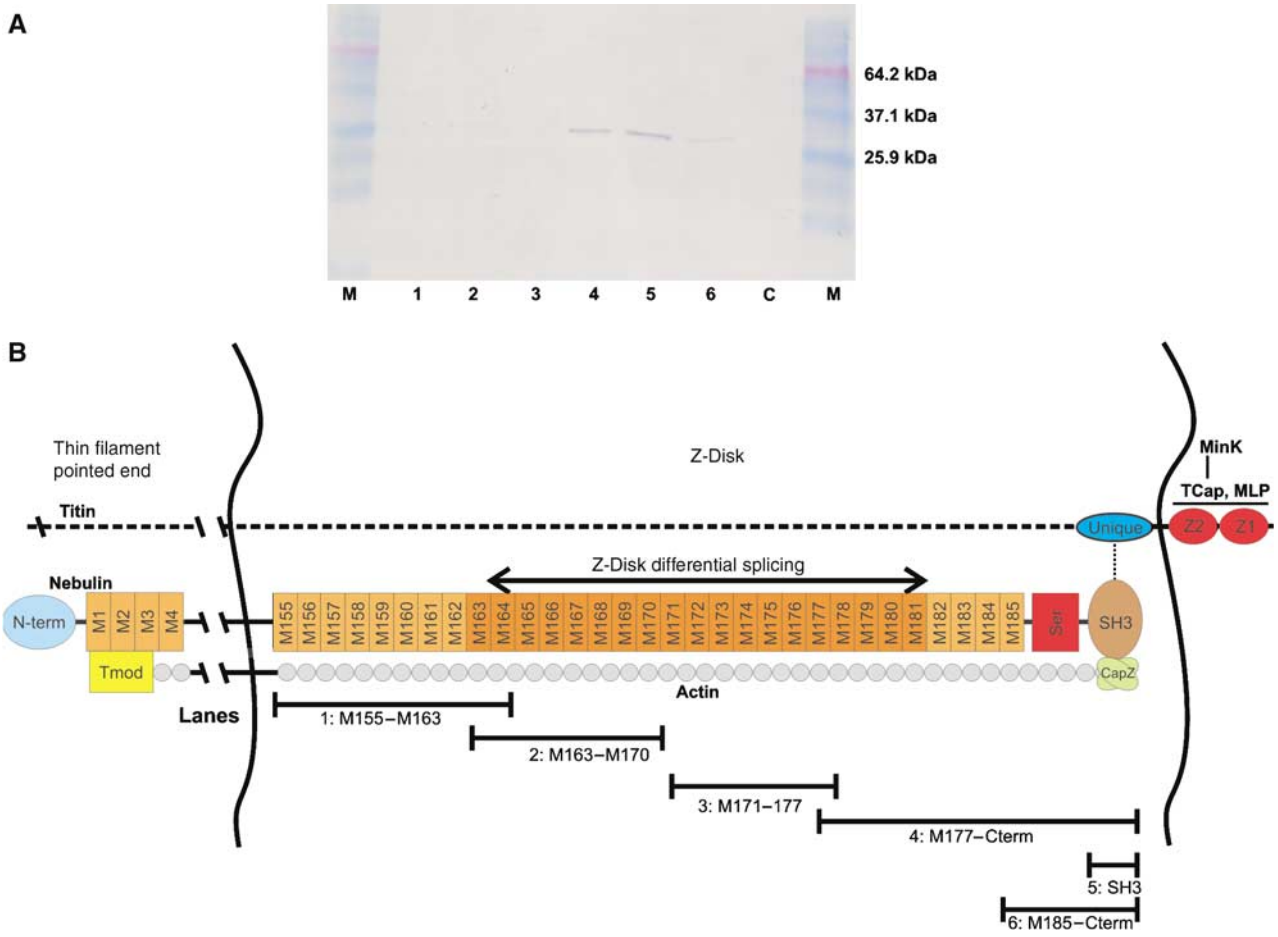

Figure 9 Interaction between nebulin M185-C-term and CapZ. (**A**) Interaction of nebulin M185–Cterm with CapZ. Six different histidine-tagged nebulin C-terminal fragments (region M155–Cterm) were co-expressed with nontagged CapZ in *E. coli* (lane 1: M155–163; lane 2: M163–170; lane 3: M171–177; lane 4: M177–Cterm; lane 5: SH3; lane 6: M185–Cterm; the fragments are also indicated at the bottom of (**B**)). After lysis of cells, soluble supernatants were purified over Ni-NTA agarose. Western blots with anti-CapZ antibody detect that CapZ co-elutes with constructs 4–6 (i.e. region M185-C-term). Lane 7: Lane marked 'C' contains cells that expressed CapZ construct alone. (B) Model for nebulin's role in Z-disks. Nebulin's C-terminal SH3 domain interacts with both CapZ and with titin, attaching thin filament barbed ends in the periphery of the Z-line. The differential expression of nebulin repeats M163–M181 may set different Z-line widths. Bars show size of expressed proteins used in lanes 1–6 of (A).

with about 100 nm wide Z-disks, see Luther and Squire (2002) and Luther *et al* (2003)) and quadriceps muscle (rich in fast fibers with about 50 nm wide Z-disks), this demonstrated the striking differential expression of six nebulin exons from the Z-disk encoding region (Figure 8D, bottom).

For testing the interaction between nebulin and CapZ, we co-expressed a bi-cistronic CapZ plasmid harboring both α- and β-CapZ subunits (Soeno *et al*, 1998) with nebulin C-terminal fragments. CapZ co-purified with those nebulin fragments harboring the region M185–Cterm (see Figure 9). In summary, our *in vitro* binding studies demonstrate that nebulin's C-terminal region (M185–Cterm) interacts with both CapZ and with titin. Therefore, the two ruler molecules implied in Z-disk width specification, titin and nebulin, are linked.

Discussion

Nebulin as a molecular ruler of the thin filament

The availability of the NEB KO mouse model with mice that are viable allows, for the first time, study of skeletal muscle myofibrils that are nebulin-deficient. In particular, measuring thin filament lengths in the NEB KO mouse allows testing, in an *in vivo* context, of the molecular ruler hypothesis proposed ~15 years ago (Kruger *et al*, 1991; Labeit *et al*, 1991). For skeletal muscle, our data indicate that nebulin is indeed required for specifying and maintaining thin filament lengths with the precision achieved *in vivo*. As for the mechanism by which nebulin controls thin filament length in skeletal muscle, we take guidance from earlier *in vitro* studies. Earlier studies suggested that since nebulin promotes actin nucleation and actin filament stability (Chen *et al*, 1993), thin filaments assembled in nebulin's presence will be longer when nebulin is absent (Figure 5E). Once polymerization has reached nebulin's amino-terminus, interaction of nebulin with Tmod will cap the thin filament (McElhinny *et al*, 2001). Thus, our working model is that nebulin is guiding and facilitating actin polymerization (internal super-repeats) as well as terminating polymerization (end regions).

With regard to cardiac muscle, it has been suggested that the low levels of nebulin expressed in myocardium could regulate thin filament lengths by novel mechanisms. One such mechanism states that nebulin can rapidly dissociate from the thin filament and then interact with another and

thereby specify the length of many thin filaments. An alternative is the so-called cap-locator mechanism that also does not require stoichiometric ratios of thin filaments and nebulin (for details, see McElhinny *et al*, 2005; Fowler *et al*, 2006; Horowits, 2006). Our Western blot results, however, failed to detect any nebulin in myocardium of both wt and KO mice. These results do not rule out that findings reported by McElhinny *et al* (2005) are correct, because they are largely based on cell culture experiments and it is possible that in cultured cardiac myocytes, expression programs are turned on that include nebulin, and that are absent *in vivo*. Furthermore, it is also possible that low-level expression of nebulin in mouse myocardium can be detected by RT–PCR or immunofluorescence (as reported by Kazmierski *et al*, 2003), but not by Western blots because of their more limited sensitivity. By loading a dilution series of skeletal muscle sample, we determined that the detection limit for skeletal muscle nebulin is reached when loading 1% of the total myofibrillar protein used for cardiac Western blots (results not shown). Thus, if cardiac muscle expresses 1% or less of the skeletal muscle nebulin level, it would go undetected. This places in cardiac muscle the upper limit for the number of nebulin filaments at 1 per 50 thin filaments (as opposed to 2 per 1 filament in skeletal muscle). We conclude that this is inconsistent with nebulin working as a ruler molecule in cardiac muscle, and propose that nebulin-independent mechanisms are likely to exist in cardiac muscle. Thus, further work is required to establish the mechanism for thin filament length control in the heart.

Nebulin and titin in Z-disks

Our studies also indicate that the functions of nebulin extend beyond thin filament length control and include controlling contractility, and specification of Z-disk structure. With regard to nebulin's role in Z-disks, both *in vivo* data from the NEB KO as well as *in vitro* binding studies support an important role of nebulin in the specification of Z-disk structure. So far, only titin has been implicated in Z-disk assembly and width control, because the differential splicing of titin's Z-repeats appears to correlate with Z-disk widths (heart expresses seven copies of titin Z-repeats; slow skeletal muscles six copies and fast skeletal muscles four copies; see Gautel *et al*, 1996; Young *et al*, 1998; Sorimachi *et al*, 1997). However, this alone appears to be insufficient to explain the extensive variations in Z-disk width (Luther and Squire, 2002; Luther *et al*, 2003). Moreover, titin's 4 to 7 α-helical 45-residue Z-repeats are too short to span Z-disks (Pfuhl *et al*, 1994). In contrast, nebulin shows extensive splice diversity within its C-terminal Z-disk region (Figure 8D). Both the differential expression of nebulin and titin Z-disk isoforms as well as the direct interaction between nebulin's C-terminus and titin's N-terminal Z-is1 domain raises the intriguing possibility that the two ruler molecules together specify Z-disk width (Figure 9). Based on its extensive splice isoform variability, we speculate that nebulin could be most important in specifying Z-disk width (Figure 8D). Interestingly, Z-is1 appears to be differentially phosphorylated during myogenesis (Gautel *et al*, 1996), suggesting that interesting developmental control mechanisms may exist. Close to nebulin's binding site for titin, nebulin also interacts with CapZ (Figures 4 and 9). We speculate that the ternary interaction of titin, nebulin and CapZ is an important rate-limiting step in myofibrillogenesis since the assembly of this complex will link together the two ruler molecules likely to specify thin and thick filament lengths (i.e. nebulin and titin) with CapZ (specifying barbed-ends, see Schafer and Cooper, 1995).

Murine and human nemaline myopathy (NM)

Human NM is the most common nondystrophic congenital myopathy with an estimated frequency of 0.02 per 1000 live births (Wallgren-Pettersson *et al*, 2004), and characterized by muscle weakness and hypotonia. Histologically, so-called 'nemaline' bodies (or 'rods') are diagnostic hallmarks. Clinically, human NM is heterogeneous and at the genetic level five genes have been implicated in NM, ACTA1, NEB, TPM2, TPM3, and TNNT1 (for a review, see Sanoudou and Beggs, 2001). For the dominant sporadic form caused by a point mutation in TPM3, a transgenic mouse model has been developed that expresses mutant TPM3 and contains nemaline rod-like structures in its skeletal muscles (Corbett *et al*, 2001). The main form of NM accounting for about half of the NM cases results from mutations in the nebulin gene (Pelin *et al*, 1999; Sanoudou and Beggs, 2001), with most mutations causing a deletion of the carboxyterminal region of nebulin (Wallgren-Pettersson *et al*, 2002). Therefore, the NEB KO mouse is a model for the main form of NM, and is likely to be valuable for gaining insights into the disease mechanisms acting in human NM. This notion is supported by the shared gene set dysregulated in human and NEB KO murine NM. Previously, the transcriptomes from 12 different NM patients ranging from the severe congenital form to mild adult cases were determined (Sanoudou *et al*, 2003). This identified the upregulation of calcium level regulating factors (eight-fold upregulation of S100A4), and the downregulation of glycogen metabolism enzymes, such as phosphorylase kinase). Intriguingly, these changes are also present in our murine model (for S100A4 eight-fold upregulation, for phosphorylase kinase α-1 (PHKA1), five-fold downregulation, see Figure 3C).

With regard to contractility, our studies suggest as potential patho-mechanism that nebulin depresses the maximal active tension by reducing filament overlap. In addition, nebulin appears to enhance crossbridge cooperativity in skeletal muscle, that is in the NEB KO the calcium dependent recruitment of crossbridges is perturbed as indicated by the reduced Hill coefficient. Altered contractility in the nebulin KO mouse is also suggested by the upregulation of sarcolipin ($70\times$). Sarcolipin is a modulator of skeletal muscle contractile force that diminishes sarcoplasmic reticulum Ca^{2+} stores by inhibiting sarcoplasmic reticulum Ca^{2+} ATPase (SERCA) function (Tupling *et al*, 2002). Considering the unexplained severe muscle weakness seen in NM patients, it is important to study the role of sarcolipin in NM.

Finally, our *in vitro* interaction data raise the possibility that the Z-disk pathology and nemaline rod formation in NM is the consequence of the perturbed interaction of nebulin with CapZ, causing an impaired capping of thin filaments at their barbed ends. We speculate that this allows the barbed end to continue to grow beyond the Z-disk and overlap with thin filaments of opposite polarity (in the adjacent sarcomere) and that this triggers recruitment of additional Z-disk proteins, resulting in wide Z-disks.

In summary, the nebulin KO mouse model described here allows to address the *in vivo* roles of nebulin for the first time. In addition to the suspected function of nebulin for pointed

end thin filament length regulation in skeletal muscle, nebulin is also an important regulator of Z-disk structure and barbed end capping, and, furthermore, it regulates contractility of skeletal muscle contraction. Importantly, the NEB KO mouse will likely aid in unravelling the molecular mechanisms of nemaline myopathy. Future studies are warranted to determine whether dysregulated calcium homeostasis, loss of myopalladin from the Z-disk, and impaired thin filament capping contribute to the severe and progressive pathology in human NM.

Materials and methods

Generation of NEB KO animals

Destruction of the TATA motif and murine nebulin exon 1 including the start ATG was achieved by homologous recombination. The recombination sequences for the vector (pTV0) were generated by long proof-reading PCRs (Takara LA Taq) (for details see Witt *et al*, 2001). Three mice lines were raised from three independent positive ES-cell clones (IB10).

Expression profiling (RT–PCR and Affymetrix gene chip analysis)

It was performed as described previously (Witt *et al*, 2004, 2005). For further details, see Supplementary data 3 (S3).

Gel electrophoresis and Western blotting

Myofibrillar proteins were extracted from day 5 and day 10 mice, separated by gel-electrophoresis and blotted essentially as described previously (Cazorla *et al*, 2000; Lahmers *et al*, 2004). For antibody detection of proteins see section 'Protein interaction studies'.

IF and IEM

NEB KO and wt mice were killed at day 14, and quadriceps muscle was stretched, frozen and sectioned using routine methods.

For EM, whole tibialis cranialis muscles were dissected from NEB KO, wt, and ht 10-day-old mice. Fibers were skinned, fixed in 3.7% paraformaldehyde labelled overnight with phalloidin-biotin (Molecular Probes, B7474, biotin-XX phalloidin), followed by streptavidin-nanogold (Nanoprobes, 2016, nanogold streptavidin conjugate), silver enhancement as per instructions with Nanogold HQ silver kitfixing, and embedding (Trombitas and Granzier, 1997). For further details on antibodies, immuno-labelling, confocal and EM microscopy, see Supplementary data S3.

For mechanical studies on fibers, skinned tibialis cranialis muscle from 10-day-old KO and wt animals were used after skinning in relaxing solution (RS) containing 1% (w/v) Triton X-100 for 6 h at ~4°C. For further details on physiology, see Supplementary data S3.

Yeast two-hybrid screens—interaction of nebulin and titin

A fragment encompassing exons 4–7 of human titin (corresponding to the Ig domain Z2 and the unique domain Z-is1; Labeit and Kolmerer, 1995a) was PCR-amplified from total human skeletal muscle cDNA with Ex4-S and Ex-7R:

(Ex-4S: tttccatgGCACCACCCAACTTCGTTCAACGACTG); (Ex-7R: tttggatcctaCACCTCTTTAGCACCAGTGGCAACAGC).

The fragment was inserted into bait vector pGBKT7 (BD Bioscience). For further details on the Y2H screen, see Supplementary data S3.

Expression in Escherichia coli and protein interaction studies

Nebulin fragments were cloned into pET-M11 and expressed in BL21 cells (Studier *et al*, 1990) either alone or co-expressed with avian CapZ in pET3d (Soeno *et al*, 1998). For details on expression of C-terminal nebulin fragments, co-purification with CapZ, and interaction with titin on SPOTS blots and in ITC, see Supplementary data S3.

Supplementary data

Supplementary data are available at *The EMBO Journal* Online.

Acknowledgements

We thank Ms Germaine Wright, Ms Caroline Benoist, Ms Xiuju Luo, Mr Chi Fong, Dr Vladimir Rybin for outstanding technical assistance. We are greatly indebted to Dr Christian Clasen for his initial work on establishing a the nebulin KO model. Thanks to Dr Carol Gregorio for providing Nebulin N-term antibodies, and Dr T Obinata for CapZ bi-cistronic pET3d expression construct. This work was supported by DFG (LA1969/1-1 and LA668/7-2) and NIH (HL062881/HL061497).

References

Bang ML, Mudry RE, McElhinny AS, Trombitas K, Geach AJ, Yamasaki R, Sorimachi H, Granzier H, Gregorio CC, Labeit S (2001) Myopalladin, a novel 145-kilodalton sarcomeric protein with multiple roles in Z-disc and I-band protein assemblies. *J Cell Biol* **153:** 413–427

Cazorla O, Freiburg A, Helmes M, Centner T, McNabb M, Wu Y, Trombitas K, Labeit S, Granzier H (2000) Differential expression of cardiac titin isoforms and modulation of cellular stiffness. *Circ Res* **86:** 59–67

Chen MJ, Shih CL, Wang K (1993) Nebulin as an actin zipper. A two-module nebulin fragment promotes actin nucleation and stabilizes actin filaments. *J Biol Chem* **268:** 20327–20334

Clark KA, McElhinny AS, Beckerle MC, Gregorio CC (2002) Striated muscle cytoarchitecture: an intricate web of form and function. *Annu Rev Cell Dev Biol* **18:** 637–706

Corbett MA, Robinson CS, Dunglison GF, Yang N, Joya JE, Stewart AW, Schnell C, Gunning PW, North KN, Hardeman EC (2001) A mutation in alpha-tropomyosin(slow) affects muscle strength, maturation and hypertrophy in a mouse model for nemaline myopathy. *Hum Mol Genet* **10:** 317–328

Fowler VM, McKeown CR, Fischer RS (2006) Nebulin: does it measure up as a ruler? *Curr Biol* **16:** R18–R20

Gautel M, Goulding D, Bullard B, Weber K, Furst DO (1996) The central Z-disk region of titin is assembled from a novel repeat in variable copy numbers. *J Cell Sci* **109** (Part 11)**:** 2747–2754

Getsios S, Huen AC, Green KJ (2004) Working out the strength and flexibility of desmosomes. *Nat Rev Mol Cell Biol* **5:** 271–281

Gregorio CC, Weber A, Bondad M, Pennise CR, Fowler VM (1995) Requirement of pointed-end capping by tropomodulin to maintain actin filament length in embryonic chick cardiac myocytes. *Nature* **377:** 83–86

Horowits R (2006) Nebulin regulation of actin filament lengths: new angles. *Trends Cell Biol* **16:** 121–124

Kazmierski ST, Antin PB, Witt CC, Huebner N, McElhinny AS, Labeit S, Gregorio CC (2003) The complete mouse nebulin gene sequence and the identification of cardiac nebulin. *J Mol Biol* **328:** 835–846

Knoell R, Hoshijima M, Hoffman HM, Person V, Lorenzen-Schmidt I, Bang ML, Hayashi T, Shiga N, Yasukawa H, Schaper W, McKenna W, Yokoyama M, Schork NJ, Omens JH, McCulloch AD, Kimura A, Gregorio CC, Poller W, Schaper J, Schultheiss HP, Chien KR (2002) The cardiac mechanical stretch sensor machinery involves a Z disc complex that is defective in a subset of human dilated cardiomyopathy. *Cell* **111:** 943–955

Kruger M, Wright J, Wang K (1991) Nebulin as a length regulator of thin filaments of vertebrate skeletal muscles: correlation of thin filament length, nebulin size, and epitope profile. *J Cell Biol* **115:** 97–107

Labeit S, Gibson T, Lakey A, Leonard K, Zeviani M, Knight P, Wardale J, Trinick J (1991) Evidence that nebulin is a protein-ruler in muscle thin filaments. *FEBS Lett* **282:** 313–316

Labeit S, Kolmerer B (1995a) The complete primary structure of human nebulin and its correlation to muscle structure. *J Mol Biol* **248:** 308–315

Labeit S, Kolmerer B (1995b) Titins: giant proteins in charge of muscle ultrastructure and elasticity. *Science* **270:** 293–296

Labeit S, Lahmers S, Burkart C, Fong C, McNabb M, Witt SH, Witt CC, Labeit D, Granzier H (2006) Expression of distinct classes of titin isoforms in striated and smooth muscles by alternative splicing, and their conserved interaction with filamins. *J Mol Biol* (in press)

Lahmers S, Wu Y, Call DR, Labeit S, Granzier H (2004) Developmental control of titin isoform expression and passive stiffness in fetal and neonatal myocardium. *Circ Res* **94:** 505–513

Littlefield R, Almenar-Queralt A, Fowler VM (2001) Actin dynamics at pointed ends regulates thin filament length in striated muscle. *Nat Cell Biol* **3:** 544–551

Luther PK, Padron R, Ritter S, Craig R, Squire JM (2003) Heterogeneity of Z-band structure within a single muscle sarcomere: implications for sarcomere assembly. *J Mol Biol* **332:** 161–169

Luther PK, Squire JM (2002) Muscle Z-band ultrastructure: titin Z-repeats and Z-band periodicities do not match. *J Mol Biol* **319:** 1157–1164

McElhinny AS, Kazmierski ST, Labeit S, Gregorio CC (2003) Nebulin: the nebulous, multifunctional giant of striated muscle. *Trends Cardiovasc Med* **13:** 195–201

McElhinny AS, Kolmerer B, Fowler VM, Labeit S, Gregorio CC (2001) The N-terminal end of nebulin interacts with tropomodulin at the pointed ends of the thin filaments. *J Biol Chem* **276:** 583–592

McElhinny AS, Schwach C, Valichnac M, Mount-Patrick S, Gregorio CC (2005) Nebulin regulates the assembly and lengths of the thin filaments in striated muscle. *J Cell Biol* **170:** 947–957

Miller MK, Bang ML, Witt CC, Labeit D, Trombitas C, Watanabe K, Granzier H, McElhinny AS, Gregorio CC, Labeit S (2003) The muscle ankyrin repeat proteins: CARP, ankrd2/Arpp and DARP as a family of titin filament-based stress response molecules. *J Mol Biol* **333:** 951–964

Morris EP, Nneji G, Squire JM (1990) The three-dimensional structure of the nemaline rod Z-band. *J Cell Biol* **111:** 2961–2978

Pelin K, Hilpela P, Donner K, Sewry C, Akkari PA, Wilton SD, Wattanasirichaigoon D, Bang ML, Centner T, Hanefeld F, Odent S, Fardeau M, Urtizberea JA, Muntoni F, Dubowitz V, Beggs AH, Laing NG, Labeit S, de la Chapelle A, Wallgren-Pettersson C (1999) Mutations in the nebulin gene associated with autosomal recessive nemaline myopathy. *Proc Natl Acad Sci USA* **96:** 2305–2310

Pfuhl M, Winder SJ, Pastore A (1994) Nebulin, a helical actin binding protein. *EMBO J* **13:** 1782–1789

Politou AS, Millevoi S, Gautel M, Kolmerer B, Pastore A (1998) SH3 in muscles: solution structure of the SH3 domain from nebulin. *J Mol Biol* **276:** 189–202

Root DD, Wang K (1994) Calmodulin-sensitive interaction of human nebulin fragments with actin and myosin. *Biochemistry* **33:** 12581–12591

Sanoudou D, Beggs AH (2001) Clinical and genetic heterogeneity in nemaline myopathy—a disease of skeletal muscle thin filaments. *Trends Mol Med* **7:** 362–368

Sanoudou D, Haslett JN, Kho AT, Guo S, Gazda HT, Greenberg SA, Lidov HG, Kohane IS, Kunkel LM, Beggs AH (2003) Expression profiling reveals altered satellite cell numbers and glycolytic enzyme transcription in nemaline myopathy muscle. *Proc Natl Acad Sci USA* **100:** 4666–4671

Schafer DA, Cooper JA (1995) Control of actin assembly at filament ends. *Annu Rev Cell Dev Biol* **11:** 497–518

Soeno Y, Abe H, Kimura S, Maruyama K, Obinata T (1998) Generation of functional beta-actinin (CapZ) in an *E. coli* expression system. *J Muscle Res Cell Motil* **19:** 639–646

Sorimachi H, Freiburg A, Kolmerer B, Ishiura S, Stier G, Gregorio CC, Labeit D, Linke WA, Suzuki K, Labeit S (1997) Tissue-specific expression and alpha-actinin binding properties of the Z-disc titin: implications for the nature of vertebrate Z-discs. *J Mol Biol* **270:** 688–695

Studier FW, Rosenberg AH, Dunn JJ, Dubendorff JW (1990) Use of T7 RNA polymerase to direct expression of cloned genes. *Methods Enzymol* **185:** 60–89

Trinick J (1994) Titin and nebulin: protein rulers in muscle? *Trends Biochem Sci* **19:** 405–409

Trombitas K, Granzier H (1997) Actin removal from cardiac myocytes shows that near Z line titin attaches to actin while under tension. *Am J Physiol* **273:** C662–C670

Tupling AR, Asahi M, MacLennan DH (2002) Sarcolipin overexpression in rat slow twitch muscle inhibits sarcoplasmic reticulum Ca2+ uptake and impairs contractile function. *J Biol Chem* **277:** 44740–44746

Vigoreaux JO (1994) The muscle Z band: lessons in stress management. *J Muscle Res Cell Motil* **15:** 237–255

Wallgren-Pettersson C, Donner K, Sewry C, Bijlsma E, Lammens M, Bushby K, Giovannucci Uzielli ML, Lapi E, Odent S, Akcoren Z, Topaloglu H, Pelin K (2002) Mutations in the nebulin gene can cause severe congenital nemaline myopathy. *Neuromusc Disord* **12:** 674–679

Wallgren-Pettersson C, Pelin K, Nowak KJ, Muntoni F, Romero NB, Goebel HH, North KN, Beggs AH, Laing NG (2004) Genotype–phenotype correlations in nemaline myopathy caused by mutations in the genes for nebulin and skeletal muscle alpha-actin. *Neuromusc Disord* **14:** 461–470

Wang K, Knipfer M, Huang QQ, van Heerden A, Hsu LC, Gutierrez G, Quian XL, Stedman H (1996) Human skeletal muscle nebulin sequence encodes a blueprint for thin filament architecture. Sequence motifs and affinity profiles of tandem repeats and terminal SH3. *J Biol Chem* **271:** 4304–4314

Wang K, Wright J (1988) Architecture of the sarcomere matrix of skeletal muscle: immunoelectron microscopic evidence that suggests a set of parallel inextensible nebulin filaments anchored at the Z line. *J Cell Biol* **107:** 2199–2212

Witt CC, Gerull B, Davies MJ, Centner T, Linke WA, Thierfelder L (2001) Hypercontractile properties of cardiac muscle fibers in a knock-in mouse model of cardiac myosin-binding protein-C. *J Biol Chem* **276:** 5353–5359

Witt CC, Ono Y, Puschmann E, McNabb M, Wu Y, Gotthardt M, Witt SH, Haak M, Labeit D, Gregorio CC, Sorimachi H, Granzier H, Labeit S (2004) Induction and myofibrillar targeting of CARP, and suppression of the Nkx2.5 pathway in the MDM mouse with impaired titin-based signaling. *J Mol Biol* **336:** 145–154

Witt SH, Granzier H, Witt CC, Labeit S (2005) MURF-1 and MURF-2 target a specific subset of myofibrillar proteins redundantly: towards understanding MURF-dependent muscle ubiquitination. *J Mol Biol* **350:** 713–722

Young P, Ferguson C, Banuelos S, Gautel M (1998) Molecular structure of the sarcomeric Z-disk: two types of titin interactions lead to an asymmetrical sorting of alpha-actinin. *EMBO J* **17:** 1614–1624